Changes in composition and lead speciation due to water washing of air pollution control residue from municipal waste incineration

Bogush, A. A., Stegemann, J. A. & Roy, A.

Published PDF deposited in Coventry University's Repository

Original citation:
Bogush, AA, Stegemann, JA & Roy, A 2019, 'Changes in composition and lead speciation due to water washing of air pollution control residue from municipal waste incineration', Journal of Hazardous Materials, vol. 361, pp. 187-199.
https://dx.doi.org/10.1016/j.jhazmat.2018.08.051

DOI 10.1016/j.jhazmat.2018.08.051
ISSN 0304-3894
ESSN 1873-3336

Publisher: Elsevier

© 2018 Published by Elsevier B.V. This is an open access article under the CC BY license (http://creativecommons.org/licenses/BY/4.0/)

Copyright © and Moral Rights are retained by the author(s) and/ or other copyright owners. A copy can be downloaded for personal non-commercial research or study, without prior permission or charge. This item cannot be reproduced or quoted extensively from without first obtaining permission in writing from the copyright holder(s). The content must not be changed in any way or sold commercially in any format or medium without the formal permission of the copyright holders.

Journal of Hazardous Materials 361 (2019) 187–199

Contents lists available at ScienceDirect

Journal of Hazardous Materials

journal homepage: www.elsevier.com/locate/jhazmat

Changes in composition and lead speciation due to water washing of air pollution control residue from municipal waste incineration

A.A. Bogush[a], J.A. Stegemann[a,*], A. Roy[b]

[a] Centre for Resource Efficiency & the Environment (CREE), Department of Civil, Environmental & Geomatic Engineering (CEGE), University College London (UCL), Chadwick Building, Gower Street, London WC1E 6BT, UK

[b] J. Bennett Johnston, Sr., Center for Advanced Microstructures & Devices, Louisiana State University, 6980 Jefferson Hwy, Baton Rouge, LA, 70806, USA

GRAPHICAL ABSTRACT

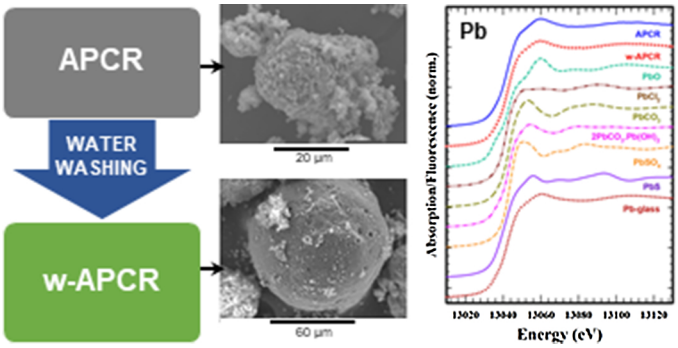

ARTICLE INFO

Keywords:
Municipal waste incinerator ash
Energy-from-Waste
EfW
Waste-to-Energy
WtE
Leaching
Extraction

ABSTRACT

Changes in elemental and mineralogical composition, and lead speciation, of air pollution control residue (APCR) from municipal solid waste incineration, due to treatment by water washing, were investigated in this work and are reported in the context of a review of the literature. Water washing was shown to substantially modify the nature of APCR by: 1) removing 23% dry mass soluble salts to disagglomerate particles and significantly reduce concentrations of the associated major elements, and increase concentrations of insoluble matrix elements and potential pollutants; and 2) respeciating elements to form new phases. X-ray absorption near edge spectroscopy (XANES) showed that the 500 mg/kg of Pb in raw and washed APCR were comprised mainly of Pb-glass, with some $PbSO_4$, and small amounts of PbO and $PbCl_2$. Semi-quantitative linear combination fitting suggests that the glass in the APCR may be unstable and release Pb under the alkaline pH of water washing, to reprecipitate as PbO. Chemical analysis suggests that some Pb may be removed by washing. Scientific understanding of the composition of raw and washed APCR, and particularly the speciation of potentially toxic metals, such as Zn and Pb, can help in developing effective element recovery and residue treatment, utilization or disposal strategies.

* Corresponding author.
E-mail address: j.stegemann@ucl.ac.uk (J.A. Stegemann).

https://doi.org/10.1016/j.jhazmat.2018.08.051
Received 15 February 2018; Received in revised form 3 August 2018; Accepted 14 August 2018
Available online 18 August 2018
0304-3894/ Crown Copyright © 2018 Published by Elsevier B.V. This is an open access article under the CC BY license (http://creativecommons.org/licenses/BY/4.0/).

1. Introduction

The generation of energy from waste (EfW) in highly engineered and controlled facilities is an effective way to recover value from municipal solid waste (MSW). Air pollution control residues (APCR) are generated in the flue gas cleaning process and include fly ash and other solid material captured before the gases are released into the atmosphere. Although they represent only 1.5–4% of the total mass of MSW combusted in modern facilities, they contain a large proportion of soluble salts, high concentrations of heavy metals, and small but measurable concentrations of toxic organic compounds (e.g., dioxin and furans) [1–5]. They are therefore considered as hazardous waste under European Waste Catalogue code 19 01 07* [6], and their appropriate management is necessary to protect the environment and human health. One of the easiest treatments for APCR is water washing to remove water-soluble phases, which has been investigated as a pre-treatment for other processes such as stabilization, thermal treatment or co-processing, at laboratory, pilot- and full-scale.

The authors have conducted previous work to gain a better understanding of the composition, mineralogy and nature of the host phases responsible for the leaching behaviour of potentially dangerous elements in APCR from UK EfW facilities [5]. The main goal of the work presented here was to investigate the effect of water washing on the particle size, elemental and mineralogical composition of APCR, with a focus on lead speciation. Scientific understanding of the composition of raw and washed APCR, and particularly the speciation of potentially toxic metals, such as Zn and Pb, can help in developing effective element recovery, and residue treatment, utilization or disposal strategies.

2. Literature review

Water washing of MSW APCR has been previously reviewed [7–10] and investigated at laboratory-scale (Table 1) by others, mainly for removal of soluble salts, such as NaCl, KCl and CaOHCl, that have the potential to cause salinization of the environment, and can cause expansion and corrosion problems in cement-based products. As noted above, APCR includes fly ash, “the particulate matter carried over from the combustion chamber and removed from the flue gas stream prior to addition of any type of sorbent materials” [1], and other solid reaction products and excess reagents (e.g., salts, lime or bicarbonate, carbon, heavy metals, dioxins and furans) captured from acid gas treatment units. Investigations conducted before the implementation of legislation to prevent emission of acid gases often studied fly ash on its own, whereas more recent work tends to be for more complex APCR that include other APCR solids. Table 1 and the Supplementary material (S1 and S2) differentiate experimental results reported for fly ash from those for more complex APCR, because these residues may have different characteristics and washing behaviour. For example, APCR from acid gas scrubbing with lime contain more Ca, Cl and SO_4, and are more alkaline than fly ash alone.

Most previous work conducted with a water leachant at ambient temperature (Table 1) focused on optimization of contact time (from 5 min to 24 h), the number of extraction steps (up to 4), and liquid-to-solid (L/S) ratio (from 0.5–100 L/kg). Short contact times at low L/S, with few steps, were preferred for better commercial viability.

The various conditions investigated resulted in a final leachate pH of 9.5 to 12.6, removal of 10–54% of the total APCR mass in the wash water, and concentration of low solubility metal salts in the solid residue. Columns 2 and 10 of Table 2 summarise the data from the sources in Table 1 (for comparison with our own work). The water washing experiments removed significant proportions of Cl^- (30–100%), SO_4^{2-} (0–94%), Na (28–89%), K (38–100%), Ca (8.0–63%), Mg (0–12%), Cr (1.3–50%) and Pb (0–19%).

The mineral phases previously identified in washed APCR (in some cases, only fly ash, as identified in Table 1) by instrumental methods are summarised in rows 1–11 of Table 3, and can be compared with a similar table for raw APCR in previous work [5]. While soluble salts (e.g., NaCl, KCl and CaClOH) generally disappeared after water washing, they sometimes remain if washing was incomplete [19,20,25]. New crystalline phases (e.g., gypsum, portlandite, and ettringite) were detected in the washed residues.

Water washing of APCR is already conducted at full scale, e.g., for recovery of gypsum in the UK by Future Industrial Services Ltd and in Denmark by Dansk Restprodukthåndtering A.m.b.a., for recovery of sodium carbonate in the Solvair process, before further treatment of APCR by cement solidification in Switzerland, chemical stabilization in Denmark [9], and before co-processing of the washed residue at Liu Li He cement plant in China.

Table 1
Parameters investigated in previous investigations of washing of from fly ash and air pollution control residues (APCR) municipal solid waste combustion.

Source number	Reference	Type (country)	Final pH	L/S	Extraction steps	Contact time, h	Mass loss, %
1	[11]	Fly ash (Italy)	10.8-11.4	25	2	0.25	NA
2	[12]	Fly ash from cyclone of a mass-burn MSW incinerator (Taiwan, ROC)	NA	2-100	1	1	NA
3	[13]	Fly ash (Italy)	NA	10	1	24	NA
4	[14]	APC residue from fluidised bed MSW incinerator (Sweden)	NA	1-2	1,3	0.083-2	18-54
5	[15]	Fly ash from electrostatic precipitator (Italy)	11.7-11.9	12.5	4	0.5	23.4
6	[7]	APCR (Spain)	12.2-12.6	0.5-10	1	1-24	NA
7	[16]	Fly ash from electrostatic precipitator (Italy)	NA	12.5	4	0.5	NA
8	[4]	APCR (UK)	12-12.6	10	1	24	NA
9	[17]	APCR (Germany/Sweden)	NA	2, 10	1	24	NA
10	[18]	Fly ash from cyclone of a mass-burn MSW incinerator (Taiwan, ROC)	9.5-10.6	2-100	1	0.5-4	NA
11	[19]	APCR from fabric filter of bubbling fluidized bed MSW incinerator with dry lime scrubber (Sweden)	12.4	50	1	24	NA
12	[20]	Fly ash from the boiler and gas quenching tower of a continuous stoker-type MSW incinerator (Japan)	NA	2-10 3	1 2	0.083 0.083, 0.17	11-15
13	[21]	APCR (Taiwan)	12.18	10	2	1.5	33
14	[22]	APCR (Italy)	NA	2-10	1	24	10-13
15	[23]	APCR (Taiwan, ROC)	NA	5	2	0.083	NA
16	[24]	APCR (Portugal)	12.1	10	1	0.17	22.2
17	[25]	APCR (Czech Republic)	NA	5, 10	1	NA	NA
18	[26]	APCR (China)	> 11.9	3-50	1	0.033-16	NA

L/S = liquid-to-solid ratio; NA indicates that a parameter was not available.

Table 2
Compositions of the raw (APCR) and washed (w-APCR) air pollution control residues from municipal solid waste combustion, with calculated element removals by washing, including comparison with the literature (more detail in S1 and S2).

Element	APCR (mg/kg dry mass)					w-APCR (mg/kg dry mass)			Removed by washing (%)			Average crustal abundance [27]
	Literature[a]		XRF	TAD	AR	XRF	TAD	AR	This work[b]	Literature[a]		
Al, %	0.32-6.4	1,2,5-18	2.2	2.5	2.2	2.7	3.4	3.3	0-5.5	< 0.01-17	2,8,11,12	8.04
Ag	NA		13	12	10	14	11	12	17-29	NA		0.05
As	< 0.05-210	1,6,8,9,14,18	5.5	12	8.2	11	15	15	0-3.8	< 0.01-8.0	8,14,18	1.5
Au	NA		NA	< 0.01	2.1	NA	0.5	1.1	NA	NA		0.0018
Ba	70-660	6,8,14,18	450	680	560	830	890	270	0	0.1-20	8,18	550
Be	317	17	NA	0.42	0.45	NA	0.7	0.48	0	NA		3.0
Bi	14	6	16	13	13	18	17	19	0-13	NA		0.127
Br	230-1100	4,12	530	NA	NA	90	NA	NA	87	NA		NA
Ca, %	10-36	1,2,4-18	35	34	30	33	28	27	25-36	8-63	2,4,8,11,12,16	3.0
Cd	6-680	1-3,5-10,13,14,16-18	30	31	31	44	36	41	0-11	< 0.01-6	1,2,5,8-10,14,16,18	0.098
Ce	13	6	11	19	15	13	23	22	6.8-9.0	NA		64
Cl, %	5.4-27	1,2,4-10,12-14,17,18	7.2	NA	NA	0.51	NA	NA	94	30-100	1-6,8,9,12-14,17,18	NA
Co	7-12	6,18	16	24	27	44	38	41	0	4-12	18	10
Cr	26-500	1-3,5-10,13,14,16-18	370	120	120	450	150	160	3.8-6.4	1.3-50	1,2,5,8,10,14,16,18	35
Cs	NA		NA	1.9	1.2	NA	0.8	0.8	68	NA		3.7
Cu	210-6200	1-3,5-14,16-18	260	230	340	390	310	420	0	< 0.01-0.5	2,8-11,14,16,18	25
Dy	NA		NA	0.9	0.9	NA	1.0	1.2	14	NA		3.5
Er	NA		NA	0.47	0.44	NA	0.59	0.70	3.3	NA		2.3
Eu	NA		NA	1.1	0.49	NA	0.58	0.68	59	NA		0.88
Fe, %	0.24-2.3	1,2,5-18	0.76	0.69	0.52	1.2	1.0	0.78	0	< 0.01-11	2,8,11,18	3.5
Ga	4.7	6	NA	5.7	5.2	NA	7.8	7.2	0	NA		17
Gd	NA		NA	1.1	1.2	NA	1.7	1.7	0	NA		3.8
Ge	NA		< 0.8	1.1	< 0.03	2.2	1.4	< 0.02	2.0	NA		1.6
Hf	NA		8.8	NA	NA	15	NA	NA	0	NA		5.8
Hg	< 0.03-110	1,3	3.2	NA	NA	1.8	NA	NA	57	NA		NA
Ho	NA		NA	0.18	0.18	NA	0.22	0.24	5.9	NA		0.8
I	NA		2.5	NA	NA	< 2.7	NA	NA	NA	NA		NA
K, %	0.9-7.3	1,2,4-17	1.0	1.0	0.89	0.37	0.45	0.32	65-72	38-100	1,2,4,5,8,11,12,16,17	2.8
La	7.3	1	8.1	17	11	12	16	16	0-28	NA		30
Mg, %	0.12-1.8	1,2,5-8,10-18	0.78	0.83	0.59	1	1.1	0.84	0-1.3	< 0.01-12	2,8,11	1.33
Mn	270-700	7-9,11,17,18	600	600	500	860	800	800	0	< 1	8,11,18	600
Mo	11	6	12	10	15	21	11	14	0-15	NA		1.5
Na, %	1.4-11	1,2,4-18	NA	1.2	1.1	NA	0.71	0.52	54	28-89	1,2,4,5,8,11,12,16,17	2.89
Nd	6.1	6	NA	7.5	7.3	NA	8.6	8.2	12	NA		26
Ni	17-160	1,5,6,14,16-18	36	50	65	54	49	80	0-25	< 0.01-24	9,14,16,18	20
P, %	0.088-2.6	2,6-8,10-13,17,18	0.37	0.35	0.31	0.54	0.5	0.48	0-6.1	< 0.01-19	2,8	0.07
Pb	640-17000	1-3,5-14,16-18	550	490	490	690	560	550	3.4-12	< 0.01-20	2,8-11,14,16,18	20
Pd	NA		NA	0.9	1.0	NA	0.5	1.0	57	NA		0.0005
Pr	NA		NA	2.3	1.9	NA	2.7	2.6	9.6	NA		7.1
Rb	78	6	21	19	18	14	12	10	49-51	NA		112
S, %	0.26-4.6	1,4,5,7,8,11-14,17,18	1.3	NA	NA	2.3	NA	NA	0	0-94	1,3-5,8,12,14,18	NA
Sb	200-500	6,8,17	200	13	180	310	14	260	0-17	< 0.01	2	0.2
Sc	NA		NA	1.6	1.6	NA	2.1	2.1	0	NA		11
Se	NA		1.9	NA	NA	3.5	NA	NA	0	NA		50
Si, %	1.1-10	1,2,5-7,10-18	3.7	NA	NA	5.0	NA	NA	0	0-4.6	2,11,12	30.8
Sm	NA		NA	1.4	1.1	NA	1.6	1.2	12	NA		4.5
Sn	200-8000	6,8,9,17	160	< 0.3	170	250	< 0.2	210	0	< 0.01	8	5.5
Sr	480	6	480	450	470	460	400	450	26-32	NA		350
Tb	NA		NA	0.39	0.25	NA	0.31	0.32	39	NA		0.64
Ti, %	0.08-0.5	6-8,11,15	0.67	0.25	0.05	0.99	0.36	0.1	0	< 0.01	8	0.3
Th	NA		6.1	2.3	1.6	8.2	2.6	2.4	0-13	NA		10.7
Tm	NA		NA	0.07	0.11	NA	0.09	0.11	1.0	NA		0.33
U	NA		42	1.0	0.8	55	1.3	1.2	0	NA		2.8
V	22-140	6,17,18	25	17	18	52	23	26	0	0.5-65	18	60
Y	NA		11	17	8	12	10	11	16-55	NA		22
Yb	NA		NA	0.64	0.59	NA	0.66	0.51	0-21	NA		2.2
Zn, %	0.22-1.0	1,2,5-14,16-18	0.29	0.33	0.27	0.38	0.43	0.36	0.06-1.1	< 0.01-3	2,8,11,14,16,18	71
Zr	58	6	110	NA	NA	170	NA	NA	0	NA		190
Total	NA		NA	NA	NA	NA	NA	NA	23	10-54		NA

NA indicates that a parameter was not available or applicable.
XRF – element analysis of solid samples by X-ray fluorescence.
TAD – element analysis of extracts from total acid digestion by inductively coupled plasma spectroscopy.
AR – element analysis of extracts from aqua regia digestion.
[a] Superscripted source numbers are defined in Tables 1 and 2 showing the element concentration ranges of fly ashes or APCR.
[b] Removal in wash water (%) = $100(C_i\text{-}C_w(1\text{-}ML))/C_i$, where C_i = initial concentration in APCR; C_w = concentration in w-APCR; ML = mass lost in washing = 0.23 kg/kg APCR; negative values caused by analytical variability but incompatible with reality have been shown as 0.

Table 3
Mineral phases previously identified in water-leached air pollution control residues from municipal solid waste combustion, compared with phases identified by X-ray diffraction in current raw (APCR) and washed (w-APCR) samples.

Source Number	Reference	$CaCO_3$ Calcite	$CaSO_4$ Anhydrite	$CaSO_4 \cdot 2H_2O$ Gypsum	$Ca_2(Mg,Al)(Al,Si)_2O_7$/ $Ca_2Al[AlSiO_7]$ Melilite/Gehlenite	SiO_2 Quartz	$Ca(OH)_2$ Portlandite	CaO Lime	$Al(OH)_3$ Gibbiste	Al_2O_3 Corrundum	NaCl Halite	KCl Sylvite	$CaCl_2 \cdot 2H_2O$	CaClOH
1	[11]	x		x										
2	[12]			x	x	x								
	[28]	x			x	x								
4	[14]	x		x			x							
5	[15]	x		x	x	x								
6	[16]	x			x	x								
11	[19]	x			x	x	x				x			
12	[20]										x	x	x	
13	[21]	x					x							x
17	[25]	x	x		x	x					x	x		
18	[26]	x		x			x							
CURRENT	w-APCR	M		M	M	M	M		M	M				
WORK	APCR	M	M		M	M		M		M	M	M		M

Source Number	$CaO \cdot Al_2O_3 \cdot CaCl_2 \cdot 10H_2O$ Friedel salts	Calcium Chloroaluminate	$Ca_6Al_2(SO_4)_3OH_{12} \cdot 26H_2O$ Ettringite	$K_2Ca(SO_4)_2 \cdot H_2O$ Syngenite	$(K,Na)_3Na(SO_4)_2$ Aphthitalite	$Ca_{10}(PO_4)_6(OH,F,Cl)_2$ Apatite	$CaAl_2Si_2O_8 \cdot 4H_2O$ Plagioclase	$KAlSi_3O_8$ – $NaAlSi_3O_8$ –$CaAl_2Si_2O_8$ Feldspar	$CaSiO_3$ Wollastonite	Ca_2SiO_4 Larnite	$Ca_5MgSiO_3O_{12}$	FeOOH Goethite	TiO_2 Rutile	Zn_2SiO_4 Willemite
1				x	x									
2								x		x	x			
						x		x					x	
4						x			x			x		
5			x											
6														
11														
12	x	x												
13														
17														
18														
CURRENT WORK			M			m								m

M and m indicate major and minor phases identified by X-ray diffraction, respectively.

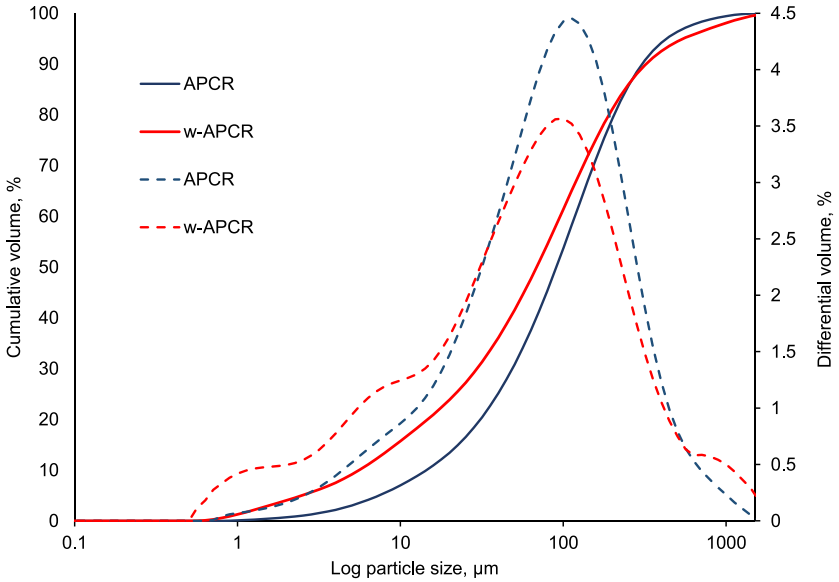

Fig. 1. Differential and cumulative particle size distributions for the raw (APCR) and washed (w-APCR) air pollution control residue.

3. Materials and methods

3.1. Air pollution control residue

A 10 kg composite sample of APCR was obtained at a single sampling time by the operator of the full-scale facility that provided samples A3, A8 and A10 used in previous work [5]. Representative subsamples of the required size for the analyses were obtained by coning and quartering.

3.2. Washed air pollution control residue

A washed APCR sample (henceforth denoted as w-APCR) was prepared by washing a subsample of APCR in deionised water at a liquid-to-solid ratio of 10 L/kg without pH adjustment (0.5 L of water with 50 g of APCR, with a final pH of 11.8). The washing conditions were based on preliminary testing, which established that as much chloride was removed after 30 min water washing, as after 24 h, which agrees with similar results from [29].

3.3. Air pollution control residue characterisation

The particle size distributions of APCR and w-APCR were measured by Malvern Mastersizer 2000 laser diffraction over the range from 0.02 μm to 2000 μm. Subsamples of the APCR and w-APCR for chemical analysis were micronised using an agate ball mill.

Total element compositions of the APCR and w-APCR were determined by three methods:

1) X-ray fluorescence (XRF) spectrometry using the Spectro X-LAB Pro 2000, which is a reliable analysis for bulk elements, but less reliable for trace elements;
2) Inductively coupled plasma optical emission spectroscopy (ICP-OES) for bulk elements and ICP-mass spectroscopy (MS) for trace elements, following:
   a Conventional "total" acid digestion with mixtures of HNO_3, H_2O_2, $HClO_4$, HF and HCl, which is used for complete analysis of bulk and trace elements; and
   b Aqua-regia digestion with 1:3 HNO_3:HCl (mol/mol), which is often used to estimate the "environmentally available" concentrations of elements in a solid, but does not release elements trapped in silicates and aluminosilicates.

X-ray powder diffraction (XRD) analysis was used to characterize the crystalline phases present in the APCR and w-APCR. Each sample was side-loaded against a ground-glass surface into a glass-backed aluminium-framed sample holder. Diffraction patterns were measured in Bragg–Brentano reflection geometry using a Bruker D8 Advance instrument. The diffractometer was equipped with a Cu anode X-ray tube (run at 40 kV, 250 mA) and an incident beam monochromator that produces a single CuKa1 line, leading to very sharp diffraction maxima. All patterns were scanned with step length 0.02° and scan speed 8°/min. Phase identification was made by matching a minimum of 3 diffraction lines to relevant diffraction patterns from the International Centre for Diffraction Data (ICDD) database using the PANanalytical proprietary software ("X'Pert HighScore Plus").

Simultaneous thermal analysis (STA) was used to investigate mass changes, and heat absorption or generation in the APCR and w-APCR in response to temperature, which are diagnostic for the phase composition. STA was performed using a NETZSCH STA 449 C instrument. Runs were conducted using about 20 mg of sample in alumina pans with a nitrogen purge gas flow rate of 100 mL/min, equilibration at 40 °C for 10 min, followed by a heating rate of 5 °C/min from 40 °C to 200 °C, and then a heating rate of 10 °C/min up to 1000 °C. An 85 μL alumina crucible and an identical empty reference crucible were used for this analysis.

The micromorphologies and compositions of the APCR and w-APCR particles, and residues remaining after their acid and aqua regia digestions, were investigated by scanning electron microscopy (SEM) at different magnifications on a JEOL JSM-6480LV high-performance, variable pressure analytical scanning electron microscope with secondary electron imaging (SEI) and backscattered electron imaging (BEI) detectors, and energy dispersive x-ray spectroscopy (EDS) with an accelerating voltage of 10 keV. Individual APCR and w-APCR particles, and compacted and polished samples were mounted rigidly on a specimen stub and coated with an ultrathin layer of carbon (graphite). More than a hundred spot analyses were performed by EDS.

Use of high resolution X-ray absorption near-edge structure spectroscopy (XANES) can give important information about element speciation for amorphous as well as crystalline materials, even if the element of interest is present at relatively low concentration. Lead speciation in the raw and washed APCR was investigated by XANES at

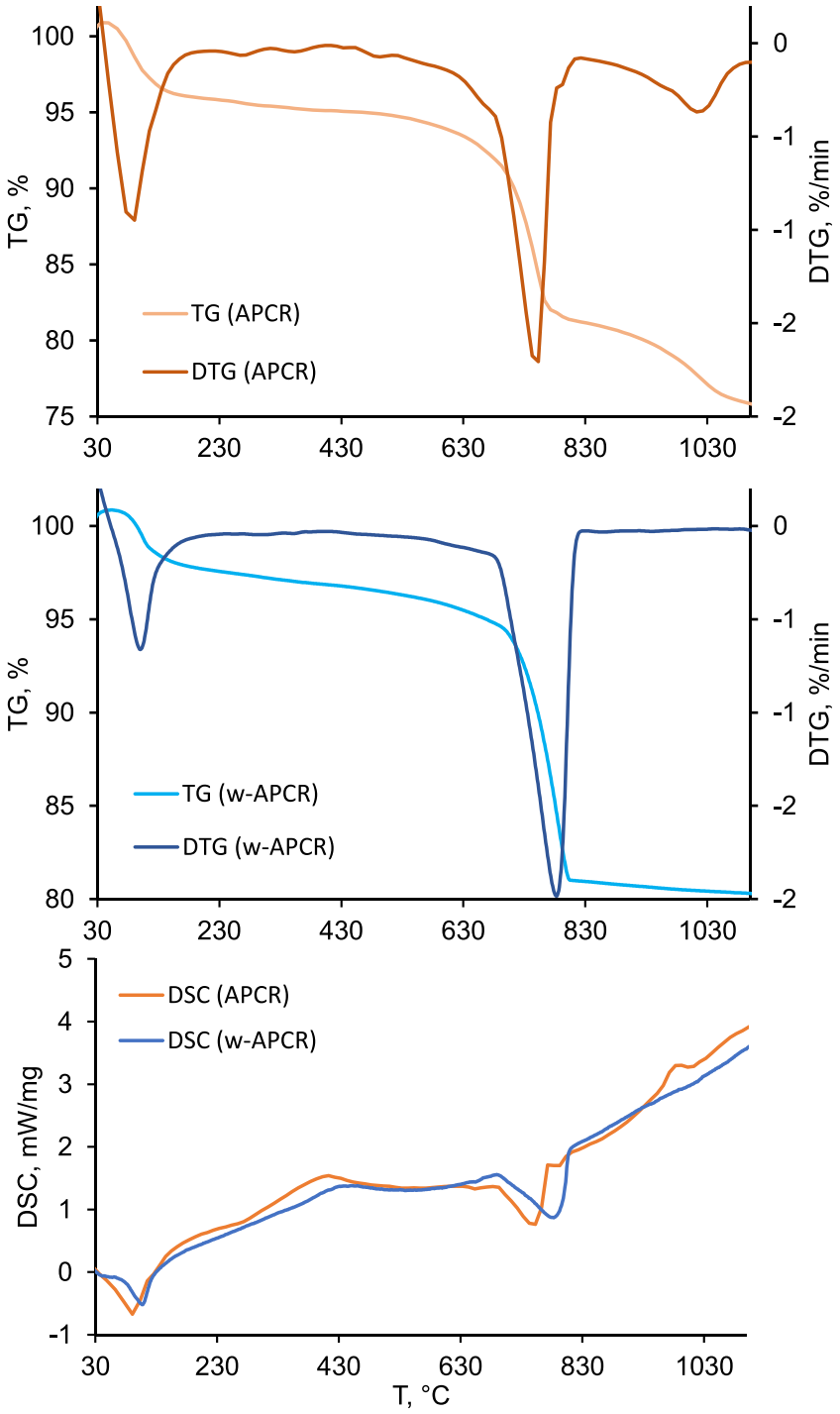

Fig. 2. Thermogravimetric, differential thermogravimetric, and differential scanning calorimetric data for raw (APCR) and washed (w-APCR) air pollution control residues from municipal solid waste combustion.

the B18 beam line at the Diamond Light Source (UK). Each sample was ground using an agate mortar and pestle, compressed into a 13 mm pellet and sealed with Kapton tape. Pb-L III edge XANES spectra were measured with a double crystal Si (111) monochromator. The monochromators were calibrated using a Pb foil. The reference materials selected for the experiments were: $PbCl_2$, PbO, $PbCO_3$, $2PbCO_3{\cdot}Pb(OH)_2$, PbS, $PbSO_4$, $PbSiO_3$, Pb-glass (Corning Glass B, NMNH 117218-1 from the Smithsonian National Museum of Natural History; 0.61% PbO). The reference material spectra were recorded in transmission mode using an ionization chamber. The sample spectra and Corning glass spectra were recorded in fluorescence mode using a 36-element Ge fluorescence detector. All spectra were measured at room temperature, and several scans (5 for transmission and 10 for fluorescence) were averaged to improve the signal-to-noise ratio. The XANES spectral analysis was performed using Athena [30]. Linear combination fitting (LCF) of the spectra for Pb in APCR and w-APCR with those of the reference materials was performed in derivative space, to identify Pb species that could have been present in the investigated samples. Extended X-ray absorption fine structure spectroscopy was not performed, because of low Pb concentrations, and because preliminary analyses

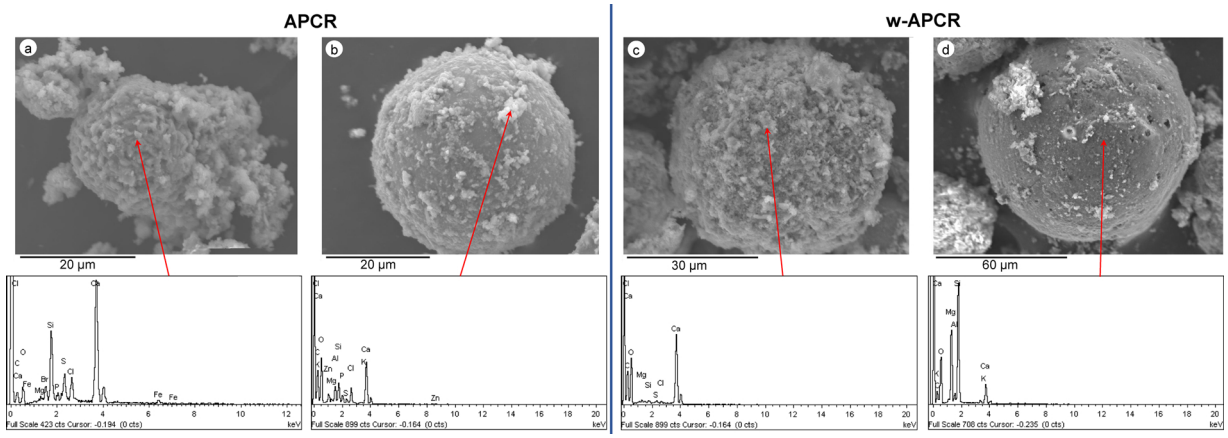

Fig. 3. Scanning electron microscopy images of raw (APCR; **a** and **b**) and washed (w-APCR; **c** and **d**) air pollution control residue with energy dispersive x-ray spectroscopy analysis.

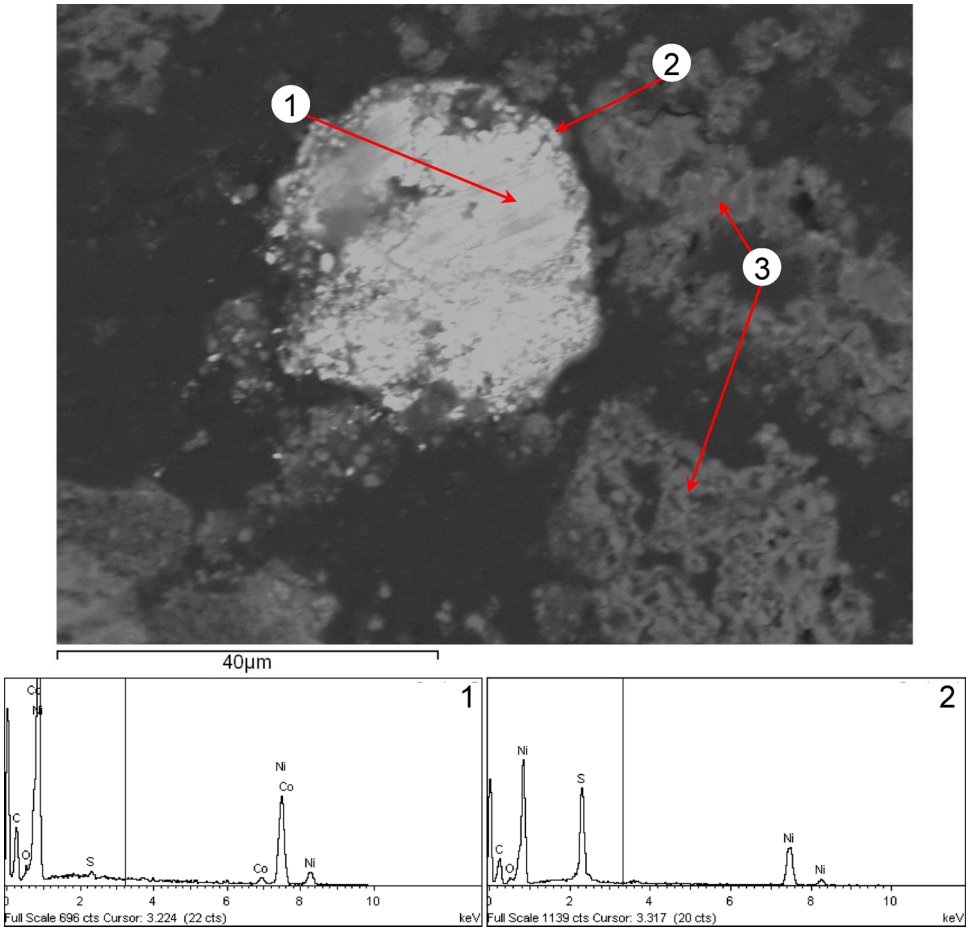

Fig. 4. Scanning electron microscopy images with backscattered electron imaging and energy dispersive x-ray spectroscopy analysis of the polished raw air pollution control residue: (1) Core of the particle with spectrum; (2) Surface area with spectrum; (3) Gel phases.

indicated poor crystallinity of Pb species.

4. Results and discussion

4.1. Particle size distribution

The particle size distribution of the APCR became multimodal after washing (Fig. 1), with an increased proportion of particles with smaller diameters. The percentage of particles smaller than 50 µm was 31% for the APCR and increased to 42% for the w-APCR. It appears that APCR particles were dissolved or disagglomerated by dissolution of water soluble phases as a result of washing.

4.2. Elemental composition

The element concentrations determined for the APCR and w-APCR

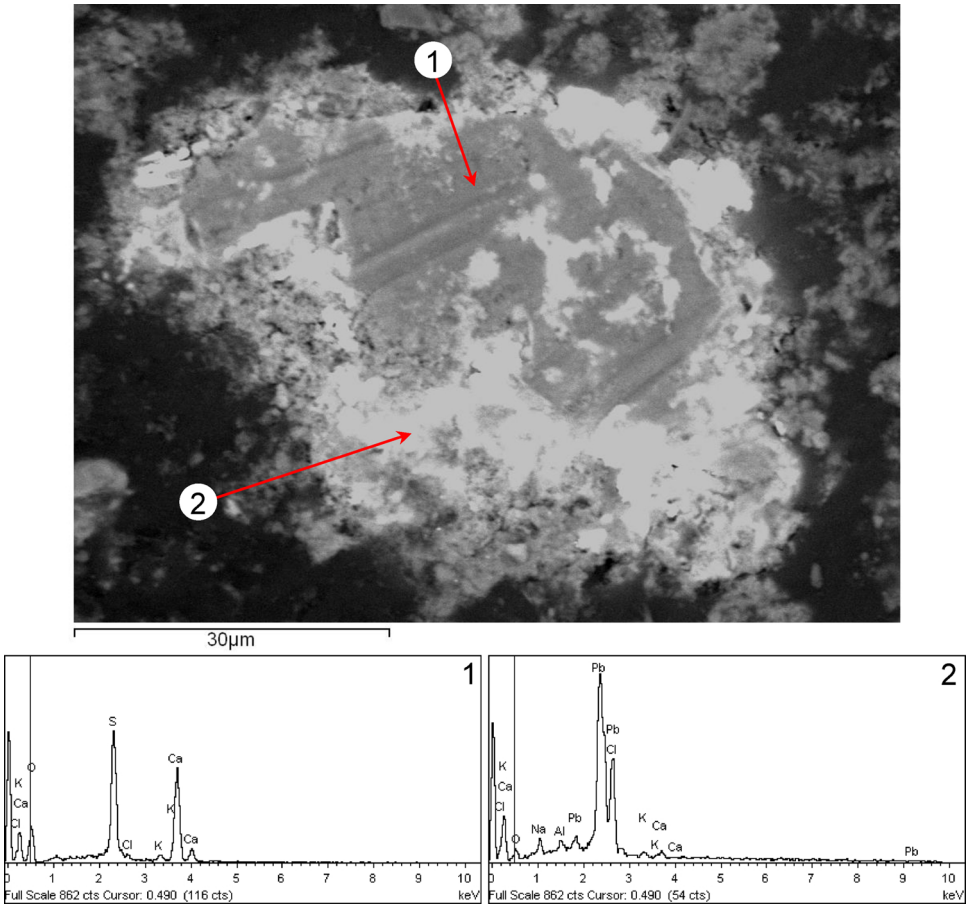

Fig. 5. Scanning electron microscopy image with backscattered electron imaging and energy dispersive x-ray spectroscopy analysis of an unshaped particle from the polished raw air pollution control residues showing (1) Ca sulphate; (2) Pb chloride hydroxide.

by XRF analysis (39 elements), and by ICP-MS and ICP-OES analysis of extracts from total and aqua-regia digestion (49 elements) are given in Table 2 (columns 3–8), in comparison with the ranges determined in APCR in the literature on washing (column 2). Major elements with > 1% dry mass in the raw APCR were Ca, Si, Al, Cl, Na, K, and S, which is consistent with the literature and our own previous observations and discussion (Bogush et al., 2015). Column 9 of Table 2 shows that removal of 23% dry mass of soluble salts by washing, including Cl (94% removal), Br (87%), alkali metals (K 65–72%; Na 54%) and alkaline earth metals (Ca 25–35%), increased proportions of the less soluble elements, yielding Ca, Si, Al, Mg, Fe, and S as the major elements in the w-APCR. Proportions of potential pollutants (e.g., Zn, Pb, Cr, Cu, Sb) also increased in the w-APCR. Although the 3–12% (15–60 mg/kg) decrease in Pb in the w-APCR is conceivably in the range of analytical error, other authors have also mentioned that a measurable proportion of Pb can be leached from APCR by water (column 10 of Table 2; [4,19,24,26]).

Residues remaining after conventional “total” acid digestion corresponded to 7.8% of the mass of the APCR and 9.4% of the mass of the w-APCR, showing that acid digestion was not able to destroy the APCR matrix completely, or that new phases may have formed during the digestion procedure, or both. SEM-EDS analysis showed that these residues were composed of very fine irregular amorphous phases (< 5 µm) and consisted mostly of Ca, Sn, P, Ti, S, and Cl with impurities of Al, Fe, Cr and Sb. Comparison of element concentrations measured in the APCR and w-APCR acid digests with results from XRF (Table 2) indicated that approximately 100% of Sn, 95% of Sb, 70% of Cr, 65% of Ti and 10–15% of Fe and P remained in the insoluble residue. 70% of Th and 98% of U were also not recovered by the acid digestion, but the concentrations of these elements were low.

Residues remaining after aqua regia digestion corresponded to ~29% of the masses of both the APCR and w-APCR; given that 23% of the APCR was removed in washing, this indicates variability in the analysis or composition of the original samples, or both. SEM showed both of these residues to contain aggregates, spherical particles, irregular, glassy, and fine phases. Aluminosilicates, including glasses of variable composition, calcium silicate, barium sulphate (probably barite), and iron and titanium oxides, were identified in both residues by EDS. Comparison of element concentrations in the APCR and w-APCR aqua regia digests with XRF results indicate that large proportions of Cr, Ti, Th, U and some Ca, Fe and P remained in the insoluble residues from aqua regia digestion, as was the case for the acid digestions. This is consistent with the minerals identified in the residues, and suggests that the environmental availability of these elements is likely to be low. In addition, about 30% of Mg was not recovered by aqua regia digestion and was observed in the silicate and aluminosilicates phases of the residues by EDS. However, it was found that Sn and Sb were completely recovered by aqua regia digestion, suggesting that these elements may be environmentally available (though not recovered by conventional “total” acid digestion). Other potential pollutants, As, Cd, Co, Cu, Mo, Ni, Pb and Zn were found to be fully recoverable by both aqua regia digestion and conventional acid digestion.

Element concentrations in the APCR and w-APCR were compared with the average upper crustal abundances of these elements [27]; final column of Table 2). The concentrations of potential pollutants, especially Zn and Pb, and also As, Cd, Co, Cr, Cu, Mo, Ni, Sb, Sn, U were found to be enriched in the APCR and w-APCR. Also, the contents of Bi and the precious metals Ag, Pd and Au in the APCR and w-APCR greatly

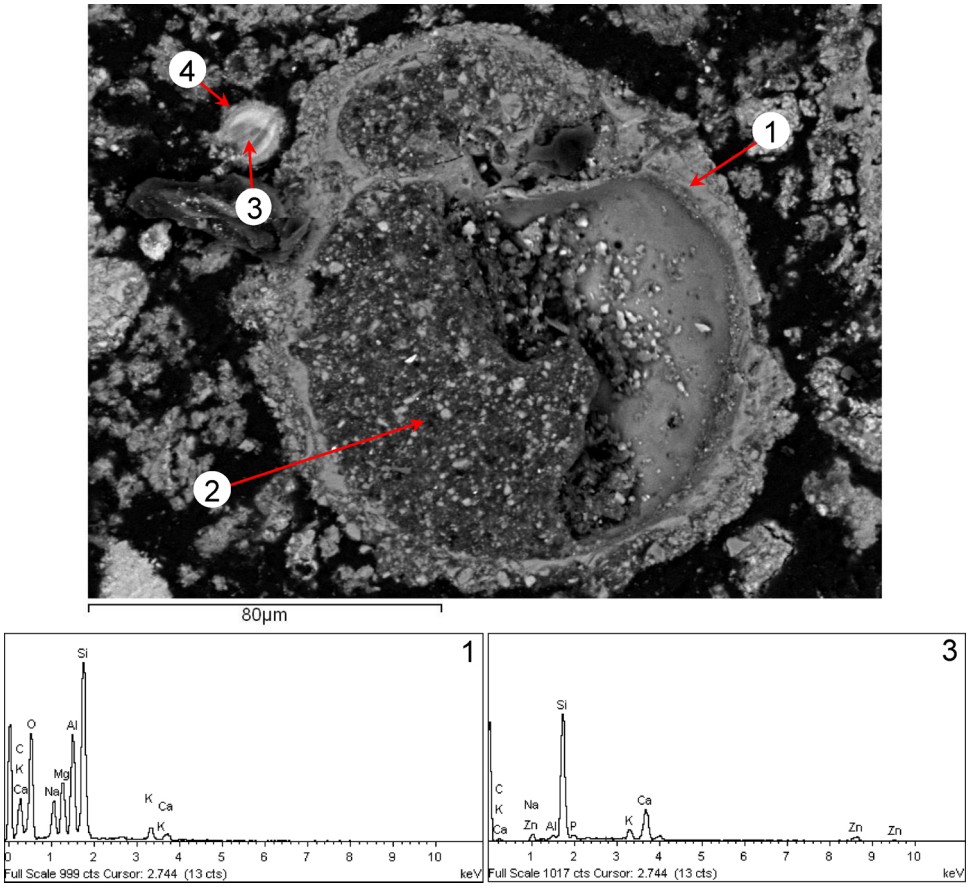

Fig. 6. Scanning electron microscopy images with backscattered electron imaging and energy dispersive x-ray spectroscopy analysis of the polished raw air pollution control residues: (1) Cenosphere shell; (2) Material inside the cenosphere; (3) Spherical particle with EDS spectrum; (4) Flakes on the surface.

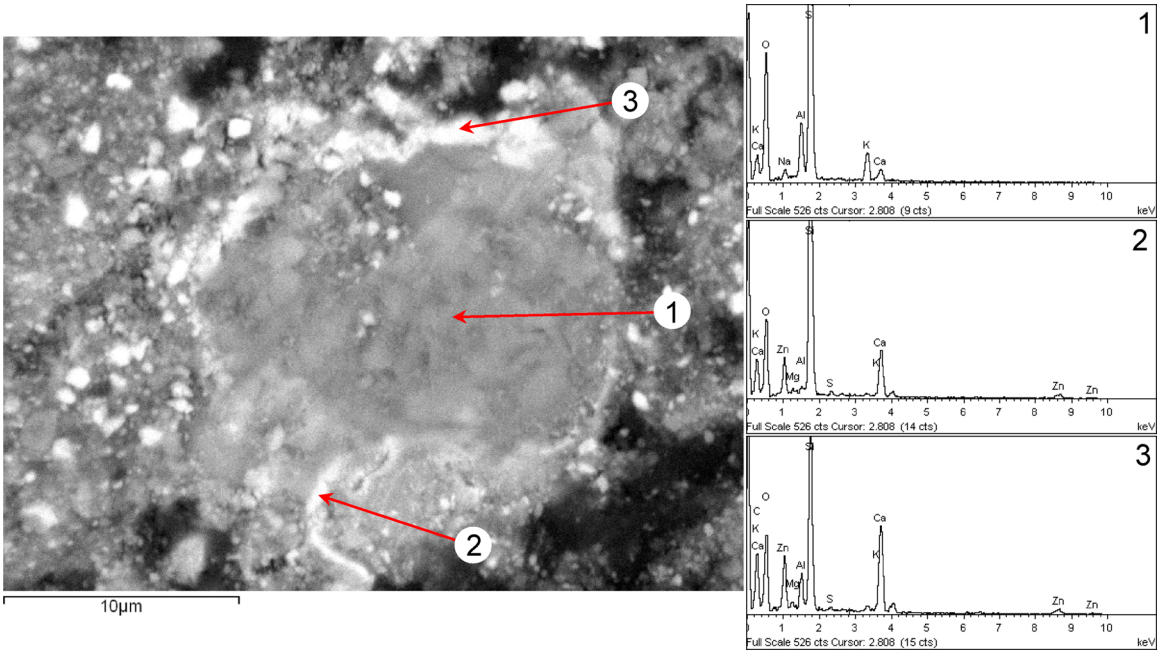

Fig. 7. Scanning electron microscopy images with backscattered electron imaging and energy dispersive x-ray spectroscopy analysis of the polished water-washed air pollution control residue: (1) Irregular particle; (2) and (3) particle rim.

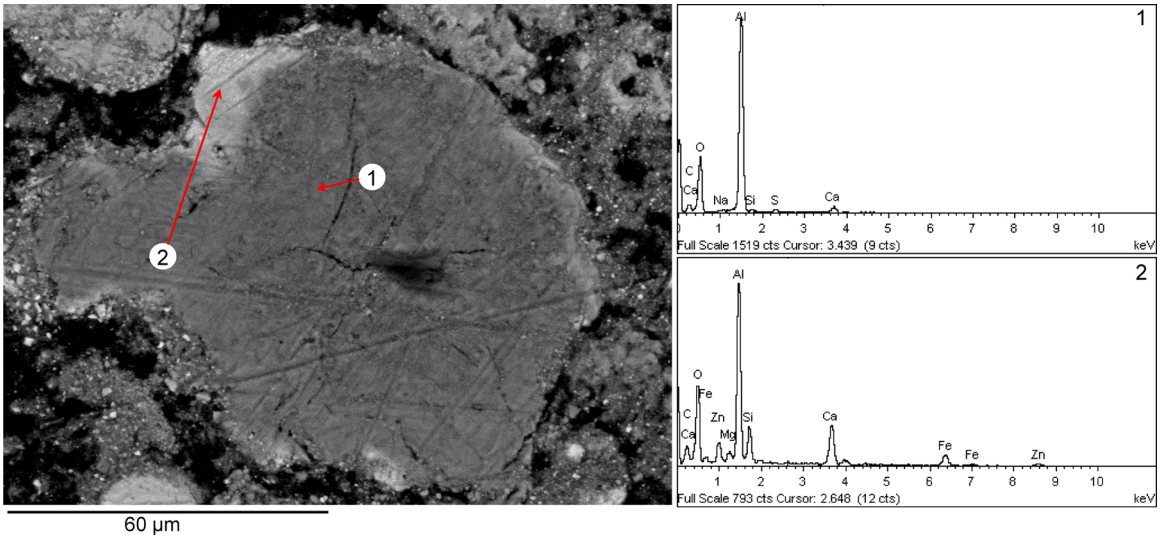

Fig. 8. Scanning electron microscopy images with backscattered electron imaging and energy dispersive x-ray spectroscopy analysis of the polished water-washed air pollution control residue: (1) Irregular particle; (2) particle edge.

exceed their average crustal abundances. Concentrations of rare earth elements, which are less volatile, were quite low in comparison with their average crustal abundance (see also [5])., 2015).

4.3. X-ray diffraction

The crystalline phases identified in the APCR and w-APCR by XRD are shown in rows 12 and 13 of Table 3. There was some amorphous material in both residues, as indicated by the background around 30–40 of 2θ and a lack of sharp peaks. The main mineral compositions of both the APCR and w-APCR generally agree with other results (see also review in Table 3 and Fig. 1 in [5]).

It is apparent that the soluble salts, including KCl, NaCl, and CaClOH, dissolved in washing, while gypsum, portlandite, gibbsite and ettringite were formed as secondary phases in the w-APCR.

4.4. Thermal analysis

The thermogravimetry (TG), differential thermal gravimetry (DTG), and differential scanning calorimetry (DSC) curves of the APCR and w-APCR are given in Fig. 2. Main mass losses of 21% for APCR and 24% for w-APCR may be observed in the interval from 30 to 1000 °C.

The first DTG peak at around 100 °C, with associated mass losses of 5.8% for the APCR and 2.2% for the w-APCR, can be observed to be an endothermic process by DSC. It is mainly due to the loss of hygroscopic moisture and dehydration of some mineral phases (e.g., gypsum, ettringite, etc.).

The DTG peak for APCR at around 470 °C corresponds to decomposition of $Ca(OH)_2$, and that at 500 °C, with a mass loss of 0.4%, is due to decomposition of CaOHCl [5]. Neither peak was observed for the w-APCR, presumably due to dissolution and amorphisation of these phases in processing.

Significant mass losses, associated with another endothermic DSC peak, were observed for both the APCR (12%) and w-APCR (15%) in the temperature range from 600 to 740 °C, consistent with the decomposition of $CaCO_3$. This peak was observed at a lower temperature for the APCR, probably due to the high content of Cl.

The APCR shows a broad exothermic peak around 1000 °C associated with a mass loss of 5.5%; it is postulated that this may be attributable to the melting and evaporation of soluble complex Na, K and Ca-containing chloride salts as well as the breakdown of the sulphate phases [5,31,32]; this peak and the associated mass loss are absent for the w-APCR sample.

4.5. Microstructure and local chemical composition

The local micromorphologies and compositions of the investigated samples determined by SEM with EDS are quite complex. The APCR and w-APCR both mainly contain aggregates, spherical particles, glass, gel and fine phases with a wide range of sizes. The main difference between these two samples is that the APCR contains highly soluble phases such as KCl, NaCl and CaClOH that were not detected in the w-APCR (Fig. 3).

SEM/EDS analysis indicated the following composition of the observed APCR phases: potassium chloride (probably sylvite), calcium chloride hydroxide, barium sulphate (probably barite), silicon oxide, different aluminosilicate glasses, calcium silicates, aluminium foil, iron and titanium oxides, and Ce, La, Nd, Th phosphates (probably monazite). Identification of the latter may seem surprising, in view of the low bulk concentrations of the rare earth elements in the APCR, but these elements were concentrated to more than 60% in some grains. Similarly, phases enriched by potential pollutants (Zn, Pb and Ni) were found in the APCR, e.g., a round particle of Ni oxide with impurities of Co (Fig. 4, point 1), with formation of Ni sulphate on its surface (Fig. 4, point 2). These particles were surrounded by gel phases consisting of calcium chloride hydroxide (Fig. 4, point 3), which was previously shown to incorporate Zn, Pb, and Cu, and may therefore play a significant role in leaching (Bogush et al., 2015). An irregular particle (about 50 µm) appeared to consist mainly of calcium sulphate (Fig. 5, point 1) and lead chloride hydroxide (Fig. 5, point 2).

Cenospheres of different sizes (50–150 µm) were also found in the APCR. The cenosphere walls mainly consist of Mg-Ca-Na-K-aluminosilicate glasses (Fig. 6, point 1). A mixture of small particles of SiO_2 and Ca-aluminosilicate glasses and gel phases of calcium chloride hydroxide was found inside the cenosphere (Fig. 6, point 2). Spherical particles of inhomogeneous composition with a size of about 10–15 µm were also observed in the APCR (Fig. 6, point 3). A bright area observed inside the sphere using BEI was identified by EDS as Ca-Zn-silicate with impurities of Al, K and P. A darker area in this sphere was mainly Ca-Zn-silicate with impurities of Al, Cl, S and P and Zn concentration (7–8 mass %) lower than in the brighter area (15–20 mass %). The surface of the spherical particle was covered by flakes of calcium sulphate (Fig. 6, point 4).

SEM/EDS analysis of the w-APCR found the composition to be similar to that of the APCR, except that chloride-containing phases had substantially dissolved, and metallic Ag could also be observed. Some phases enriched by potential pollutants (Zn and Pb) were found in the w-APCR. For example, there are many irregular particles of K-Ca-Na-

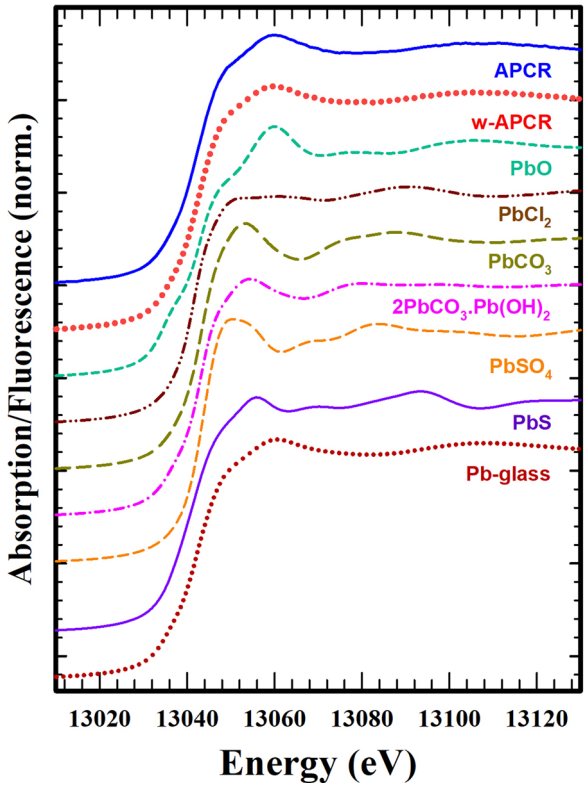

Fig. 9. Pb LIII-edge X-ray absorption near edge spectra for APCR, w-APCR, and reference materials.

Table 4
Results from linear combination fitting of the PbLIII-edge X-ray absorption near edge spectra for raw (APCR) and washed (w-APCR) air pollution control residues from municipal solid waste combustion using Athena in derivative space.

Reference	mass proportion	
Material	APCR	w-APCR
Pb-glass*	0.837	0.742
$PbCl_2$	0.018	0.018
PbO	0.026	0.066
$PbSO_4$	0.130	0.174
Total Pb	1.000	1.000
Reduced χ^2	(4.0×10^{-6})	(2.2×10^{-6})

* Corning Glass B NMNH 117218-1; 0.61% PbO.

aluminosilicate glass (e.g., Fig. 7, point 1) with rims of Ca-Zn-aluminosilicate and Ca-Zn-silicate (e.g., Fig. 7, points 1 and 2, respectively). The same particles were identified in the raw APCR but they are usually covered by fine water-soluble phases containing (presumably KCl, NaCl and CaClOH). Also, Ca-Fe-Zn-aluminate, with a Zn concentration of up to 11%, was identified in association with irregular aluminium oxide particles in the w-APCR (Fig. 8).

4.6. Pb Speciation by X-Ray absorption near edge spectroscopy

Fig. 9 shows the Pb-LIII edge XANES spectra determined for the APCR, w-APCR and relevant reference materials. The Pb-LIII edge XANES spectrum of the w-APCR shows small differences from the APCR, which suggests that Pb speciation is similar, but altered by water-washing of the APCR.

The results of linear combination fitting of the spectra for Pb in the APCR and w-APCR with the spectra for the reference compounds are presented in Table 4. Pb chloride hydroxide, which was observed by SEM/EDS in the APCR, could not be included in fitting, as a reference sample was not analysed. However, the excellent fit of the reference materials included in Table 4, demonstrated by Fig. 10, suggests that it (or other Pb compounds not examined by XANES) can only be a very minor component.

Thus, Pb in both the APCR and w-APCR appears to be speciated mainly as Pb-glass, with some $PbSO_4$, and small amounts of PbO and $PbCl_2$. The component proportions found by linear combination fitting of the XANES spectra must be considered to be semi-quantitative, but the difference in proportions of the reference materials in the best fit suggest that the highly impure and variable glass in the APCR may be unstable, such that Pb is released under the alkaline pH of the washing, to reprecipitate as PbO.

Speciation of Zn in APCR has been investigated in detail in previous work [33].

5. Conclusions

Raw APCR is a complex material, chemically comprised mainly of Ca, Si, Al, and S. These elements are found in calcite, quartz, melilite and glass, which remain after water washing, as well as anhydrite and gypsum, which are transformed to gypsum, portlandite and ettringite

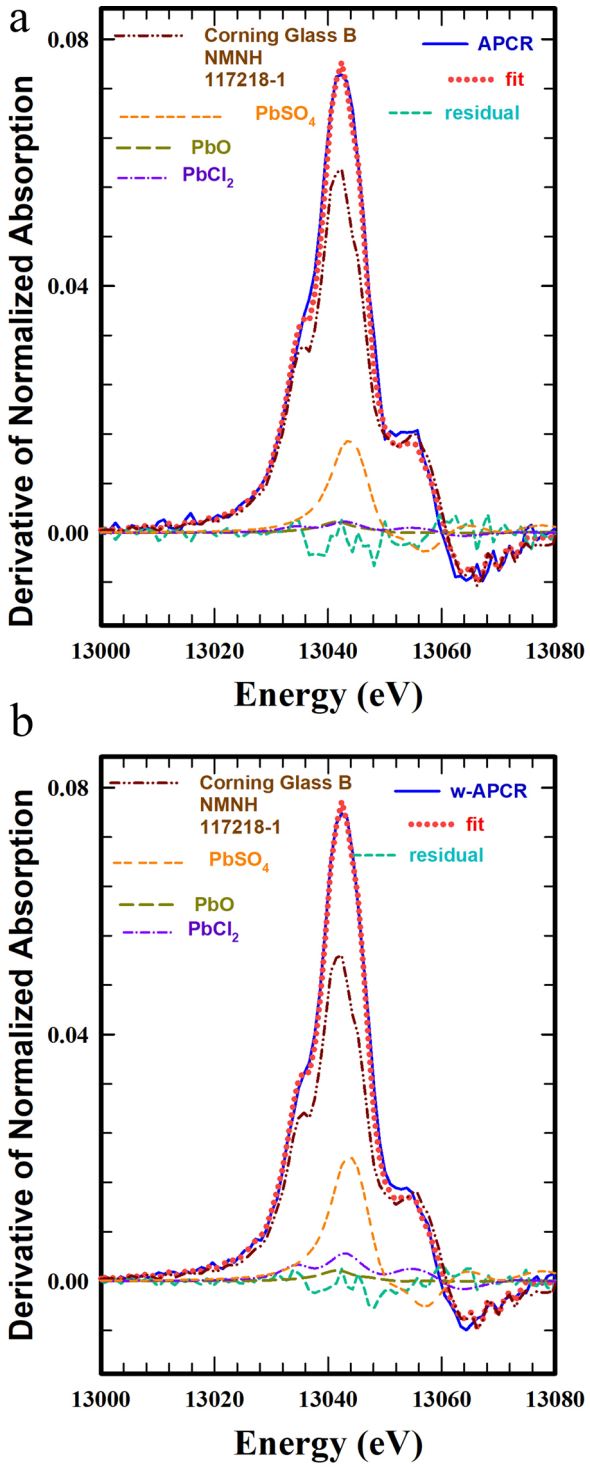

Fig. 10. Derivative Pb LIII-edge X-ray absorption near edge spectra for a) raw (APCR), and b) washed (w-APCR), air pollution control residues from municipal solid waste combustion, together with relevant reference materials, best fit and residual obtained by linear component fitting.

by washing.

Percent levels of Na, K and Cl in raw APCR, found in halite, sylvite and calcium chloride hydroxide, as well as Ca, are substantially removed by washing. Most other elements, including Al, Si, Mg, Fe and potential pollutants (e.g., Zn, As, Cd, Co, Cr, Cu, Mo, Sn, U) with complex speciation, are concentrated in the solids by washing, due to reduction of the overall mass by dissolution of the soluble salts.

XANES showed that the 500 mg/kg of Pb in the raw and washed APCR were comprised mainly of Pb-glass, with some $PbSO_4$, and small amounts of PbO and $PbCl_2$. The analysis is only semi-quantitative, but suggests that the highly impure and variable glass in the APCR may be unstable, such that Pb is released under the alkaline pH of the washing, to reprecipitate as PbO.

Precious metals (e.g., Ag, Pd and Au) are enriched in both raw and washed APCR; though concentrations are not comparable to ores, their presence suggests the potential for their recovery from separated waste streams (e.g., electronics) prior to energy recovery, or the possibility of co-extraction with more aggressive APCR processing. Rare earth

elements do not accumulate in the residues.

Acknowledgements

The authors gratefully acknowledge the valuable assistance of the following:

This work was funded by UK Engineering and Physical Sciences Research Council [Grant EP/M00337X/1, 2015-2018].

Appendix A. Supplementary data

Supplementary material related to this article can be found, in the online version, at doi:https://doi.org/10.1016/j.jhazmat.2018.08.051.

References

[1] A.J. Chandler, T.T. Eighmy, J. Hartlen, O. Hjelmar, D.S. Kosson, S.E. Sawell, H.A. Van der Sloot, J. Vehlow (Eds.), Municipal Solid Waste Incinerator Residues: Studies in Environmental Science, International Ash Working Group (IAWG), vol. 67, Elsevier Science B.V., Amsterdam, 1997.

[2] T. Astrup, C. Rosenblad, S. Trapp, T.H. Christensen, Chromium release from waste incineration air-pollution-control residues, Environ. Sci. Technol. 39 (2005) 3321–3329.

[3] M.J. Quina, J.C. Bordado, R.M. Quinta-Ferreira, Treatment and use of air pollution control residues from MSW incineration: an overview, Waste Manage. 28 (11) (2008) 2097–2121.

[4] D. Amutha Rani, A.R. Boccacchini, D. Deegan, C.R. Cheeseman, Air pollution control residues from waste incineration: current UK situation and assessment of alternative technologies, Waste Manage. 28 (11) (2008) 2279–2292.

[5] A.A. Bogush, J.A. Stegemann, I. Wood, A. Roy, Element composition and mineralogical characterisation of air pollution control residue from UK energy-from-waste facilities, Waste Manage. 36 (2015) 119–129.

[6] European Commission Decision 2000/532/EC of 3 May 2000 replacing Decision 94/3/EC establishing a list of wastes pursuant to Article 1(a) of Council Directive 75/442/EEC on waste and Council Decision 94/904/EC establishing a list of hazardous waste pursuant to Article 1(4) of Council Directive 91/689/EEC on hazardous waste.

[7] J.M. Chimenos, A.I. Fernandez, A. Cervantes, L. Miralles, M.A. Fernandez, F. Espiell, Optimizing APC residue washing process to minimize the release of chloride and heavy metals, Waste Manage. 25 (2005) 686–693.

[8] M.J. Quina, Treatment Processes and Valorization of APC Residues-municipal Solid Waste Incineration, PhD thesis University of Coimbra, Portugal, 2005.

[9] T. Astrup, Management of APC Residues From W-t-E Plants: an Overview of Management Options and Treatment Methods, ISWA-WG Thermal Treatment of Waste, Subgroup APC Residues From W-t-E Plants, second ed., Technical University of Denmark, Denmark, 2008.

[10] X. Gao, W. Wang, T. Ye, F. Wang, Y. Lan, Utilization of washed MSWI fly ash as partial cement substitute with the addition of dithiocarbamic chelate, J. Environ. Manage. 88 (2008) 293–299.

[11] T. Mangialardi, A.E. Paolini, A. Polettini, P. Sirini, Optimization of the solidificationrstabilization process of MSW fly ash in cementitious matrices, J. Hazard. Mater. B70 (1999) 53–70.

[12] K.-Sh. Wang, K.-Y. Chiang, K.-L. Lin, Ch.-J. Sun, Effects of a water-extraction process on heavy metal behavior in municipal solid waste incinerator fly ash, Hydrometallurgy 62 (2001) 73–81.

[13] C. Collivignarelli, S. Sorlini, Reuse of municipal solid wastes incineration fly ashes in concrete mixtures, Waste Manage. 22 (2002) 909–912.

[14] Z. Abbas, A.P. Moghaddam, B.M. Steenari, Release of salts from municipal solid waste combustion residues, Waste Manage. 23 (2003) 291–305.

[15] T. Mangialardi, Effects of a washing pre-treatment of municipal solid waste incineration fly ash on the hydration behaviour and properties of ash - Portland cement mixtures, Adv. Cem. Res. 16 (2) (2004) 45–54.

[16] G. De Casa, T. Mangialardi, A.E. Paolini, L. Piga, Physical-mechanical and environmental properties of sintered municipal incinerator fly ash, Waste Manage. 27 (2007) 238–247.

[17] M. Aguiar del Toro, W. Calmano, H. Ecke, Wet extraction of heavy metals and chloride from MSWI and straw combustion fly ashes, Waste Manage. 29 (2009) 2494–2499.

[18] K.Y. Chiang, C.C. Tsai, K.S. Wang, Comparison of leaching characteristics of heavy metals in APC residue from an MSW incinerator using various extraction methods, Waste Manage. 29 (2009) 277–284.

[19] K.K. Fedje, Ch. Ekberg, G. Skarnemark, B. Steenari, Removal of hazardous metals from MSW fly ash – an evaluation of ash leaching methods, J. Hazard. Mater. 173 (2010) 310–317.

[20] F. Zhu, M. Takaoka, K. Oshita, Y. Kitajima, Y. Inada, Sh. Morisawa, H. Tsuno, Chlorides behaviour in raw fly ash washing experiments, J. Hazard. Mater. 178 (2010) 547–552.

[21] W.S. Chen, F.C. Chang, Y.H. Shen, M.S. Tsia, C.H. Ko, Removal of chloride from MSWI fly ash, J. Hazard. Mater. 237–238 (2012) 116–120.

[22] F. Colangelo, R. Cioffi, F. Montagnaro, L. Santoro, Soluble salt removal from MSWI fly ash and its stabilization for safer disposal and recovery as road basement material, Waste Manage. 32 (2012) 1179–1185.

[23] Ch.-G. Chen, Ch.-J. Sun, S.-H. Gau, Ch.-W. Wu, Y.-L. Chen, The effects of the mechanical–chemical stabilization process for municipal solid waste incinerator fly ash on the chemical reactions in cement paste, Waste Manage. 33 (2013) 858–865.

[24] M.J. Quina, J.C. Bordado, R.M. Quinta-Ferreira, Recycling of air pollution control residues from municipal solid waste incineration into lightweight aggregates, Waste Manage. 34 (2014) 430–438.

[25] M. Keppert, J.A. Siddique, Z. Pavlík, R. Herný, Wet-treated MSWI fly ash used as supplementary cementitious material, Adv. Mater. Sci. Eng. 842807 (2015) 1–8.

[26] Z. Yang, S. Tian, R. Ji, L. Liu, X. Wang, Z. Zhang, Effect of water-washing on the co-removal of chlorine and heavy metals in air pollution control residue from MSW incineration, Waste Manage. 68 (2017) 221–231.

[27] S.R. Taylor, S.M. Mclennan, The geochemical evolution of the continental Crust, Rev. Geophys. 33 (2) (1995) 241–265.

[28] P. Piantone, F. Bodenan, R. Derie, G. Depelsenaire, Monitoring the stabilization of municipal solid waste incineration fly ash by phosphation: mineralogical and balance approach, Waste Manage. 23 (2003) 225–243.

[29] E. Rouchotas, C.R. Cheeseman, Metal Removal From Air Pollution Control Residues by a Water/acid Extraction Process, M.Sc. thesis Imperial College, London, 2001.

[30] B. Ravel, M. Newville, ATHENA, ARTEMIS, HEPHAESTUS: data analysis for X-ray absorption spectroscopy using IFEFFIT, J. Synchrotron Radiat. 12 (4) (2005) 537–541.

[31] D. Amutha Rani, E. Gomez, A.R. Boccaccini, L. Hao, D. Deegan, C.R. Cheeseman, Plasma treatment of air pollution control residues, Waste Manage. 28 (2008) 1254–1262.

[32] S.R. Todor, Thermal Analysis of Minerals, Abacus Press, Tunbridge Wells, 1964.

[33] A. Bogush, A. Roy, J.A. Stegemann, Speciation and Leachability of Zinc in Air Pollution Control Residues and Effects of Acid Waste Blending, Unpublished results (2018).